Synchrotron X-ray Diffraction at the APS, Sector 16 (HPCAT)

A. F. Goncharov, J. M. Zaug, J. C. Crowhurst

Lawrence Livermore National Laboratory, Livermore, CA, U.S.A.

Introduction

We present here the summary of the results of our studies using the APS synchrotron beamline IDB Sector 16 (HPCAT).

Optical calibration of pressure sensors for high pressures and temperatures

The high-pressure ruby scale for static measurements is well established [1] to at least 100 GPa (about 5% accuracy), however common use of this and other pressure scales at high temperature is clearly based upon unconfirmed assumptions. Namely that high temperature does not affect observed room temperature pressure derivatives. The establishment of a rigorous pressure scale along with the identification of appropriate pressure gauges (i.e. stable in the high P-T environment and easy to use) is important for securing the absolute accuracy of fundamental experimental science where results guide the development of our understanding of planetary sciences, geophysics, chemistry at extreme conditions, etc.

X-ray diffraction in formic acid under high pressure

Formic acid (HCOOH) is common in the solar system; it is a potential component of the Galilean satellites [2]. Despite this, formic acid has not been well-studied at high temperatures and pressures. A phase diagram of formic acid at planetary interior pressures and temperatures will add to the understanding of planetary formation and the potential for life on Europa. Formic acid (unlike most simple organic acids) forms low-temperature crystal structures characterized by infinite hydrogen-bonded chains of molecules. The behavior of these hydrogen bonds at high pressure is of great interest. Our current research fills this need.

Methods and Materials

Diffraction

The monochromatic x-ray beam was focused to a 10-15 micron diameter spot. The powder diffraction was collected on a MAR 345 electronic image plate detector.

Diamond anvil cell (DAC)

We performed a series of x-ray/optical calibaration experiments at high pressures and temperatures in order to establish correlations between different sensors. External resistively-heated DACs were used, that were equipped with two heaters and thermocouples. The temperature was measured to within ±1 K below 600 K and ±5 K above 600 K.

A sample of formic acid was treated by repeated cycling of pressure (below 15 GPa) at two temperatures (77 and 300 K). This procedure allowed us to obtain quasi-powder ring-like two-dimensional diffraction patterns, which would otherwise be spotty because of the sample texture.

Fluorescence/Raman for independent pressure determination

We developed and built a portable Raman/fluorescence system, which is compatible with concomitant x-ray measurement inside the x-ray synchrotron hutch. It consists of a remote laser (tunable sources, e.g. Ar ion laser, can be used), a Raman /fluorescence microprobe and a remote spectrograph with CCD detector, all three components coupled by optical fibers (single mode for the incident laser radiation and multimode for the signal delivery to the spectrograph). The Raman/fluorescence microprobe is a compact laser microscope (with CCD imaging camera), equipped with holographic transmission gratings, serving as a laser bandpass filter, a beamsplitter, and a notch filter, all being tunable in a wide spectral range. Due to flexibility of the optical fibers, all components of the system can be freely moved without compromising the alignment. This makes the system easy and convenient to use, especially under the conditions of synchrotron beamline operation. The system has a throughput comparable to conventional Raman/fluorescence systems. The important advantage of the system described is the possibility to tune the excitation wavelength in a relatively wide range (*e.g.*, 476-532 nm), which is important for the optimum excitation of the fluorescent pressure gauges and Raman spectra of interest. The system described has been installed at the HPCAT and has been successfully tested in the IDB hutch.

Results and Discussion

Optical calibration of pressure sensors for high pressures and temperatures

We critically examined the use at high temperature of well-known fluorescence gauges (ruby, $SrB_4O_7:Sm^{2+}$), Raman based gauges (cubic BN, C^{12}, C^{13}, and N_2) and X-ray (Au). Consequently we present data obtained from combined fluorescence, Raman, and X-ray diffraction experiments, where all six gauges were studied while under identical P-T conditions using N_2 as the pressure transducer. The effects of pressure on the temperature dependence of fluorescence intensity and spectral position in common pressure sensors used in diamond cells is measured. We chose x-ray diffraction of gold in

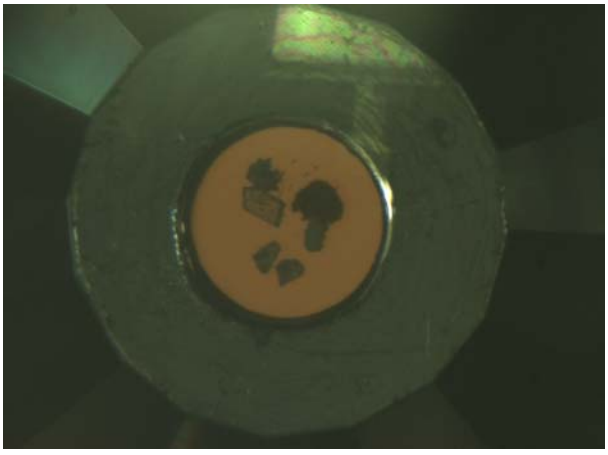

Fig. 1. Samples before loading: cBN, diamond, ruby, Au, $SrB_4O_7:Sm^{2+}$.

combination with Raman data (where temperature dependences

can be sufficiently accurately constrained) to cross check temperature derivatives of fluorescence and Raman gauges.

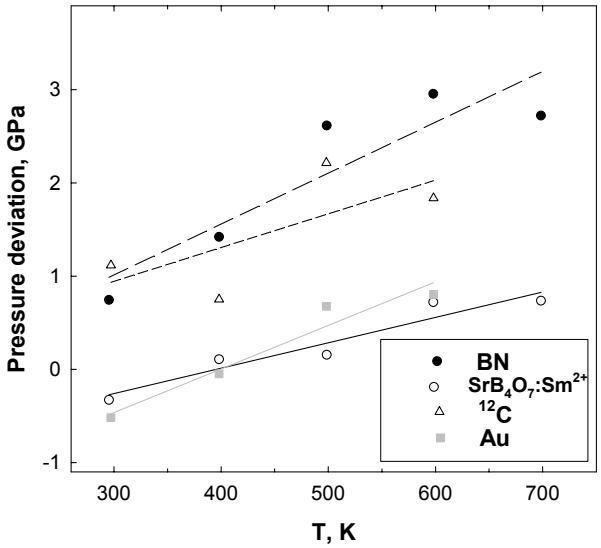

Fig. 2. Temperature dependence of the pressure deviation measured by different gauges with respect to that determined using the conventional ruby scale. Nominal pressure is in the 30-40 GPa range.

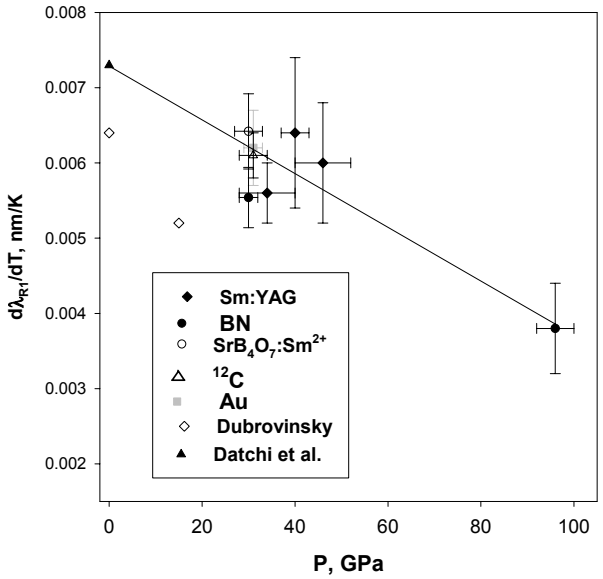

Fig. 3. Pressure dependence of the temperature derivative of the ruby R1 spectral position. The solid line is the best fit to our data determined by using different sensors (different symbols, see legend) and that of Ref. [4] at ambient pressure. Data of Ref. [5] are shown for comparison.

The results of our investigation show that there are measurable pressure-temperature cross derivatives for the ruby gauge (Fig. 2). This figure shows the results of pressure measurements using various gauges relative to the conventional ruby scale which assumes a temperature dependence that is independent of pressure. Although the data vary for different gauges, the ruby scale clearly underestimates pressure at high temperatures and nominal pressure of 32 GPa. More systematic work is required to reduce the experimental deviation. Similar results have been obtained for other pressures and also in the optical experiments with Sm^{3+}YAG and ruby optical gauges (Goncharov et al, submitted, Ref. [3]). We propose an improvement to the high-pressure ruby scale at high temperatures that consists of a pressure dependent coefficient that corresponds to the slope in the temperature dependence of the spectral position of the ruby fluorescence line. This coefficient varies from 0.0075 nm/K at ambient pressure to approximately 0.0035 nm/K at 100 GPa (Fig. 3). Thus, the ruby fluorescence scale becomes less sensitive to temperature at high pressures.

X-ray diffraction in formic acid under high pressure

Surprisingly, the crystal structure of formic acid produced under pressure was reported to be different from that at ambient pressure and low temperature. According to a single-crystal XRD study [6], it forms near dimers consisting of *cis*- and *trans*-molecules. The only Raman study of high-pressure FA (of a deuterated sample) [7] reports softening of O-D and C=O stretch bands, which indicate strengthening of the hydrogen bond. A change of slope of these bands at 4.5 GPa was interpreted as the phase transformation related to the conformational change from *cis* to *trans*. The most recent powder XRD and IR-absorption study [8] confirms the initial softening of O-H and C=O bonds and the frequency anomalies at 4.5 GPa, but finds the crystal structure to be identical to the low temperature one [9], and unchanged up to 12 GPa.

The positions and the number of Bragg reflections in our XRD patterns (Fig. 4) between 1-30 GPa correspond to those expected for the $Pna2_1$ space group of the low-temperature solid [9]. The intensities of the peaks vary in different experiments and different points of the sample. This is due to sample texturing. Thus, only a LeBail fit could be used to refine lattice parameters (Fig. 4).

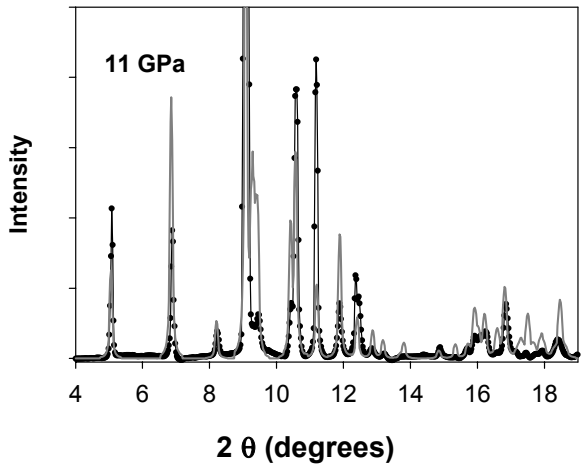

Fig. 4. XRD pattern of formic acid (λ = 0.4245 Å) at 11 GPa. Solid lines- experiment, gray line- computer generated diffraction pattern for $Pna2_1$ structure.

Significantly better quality powder diffraction (Fig. 5) patterns were obtained after back-transformation from the high-pressure phase (see below). A partial refinement (fractional coordinates of atoms were fixed) of the 4 GPa XRD pattern showed excellent agreement with the low-temperature structure, while the pattern corresponding to the *Pnma* space group [6]

clearly does not match with experimental results (Fig. 5) in positions and intensity of the Bragg peaks. Thus, we do not confirm the more complex high-pressure structure proposed in Ref. [6] (see also Ref. [8]) and the corresponding conformational change.

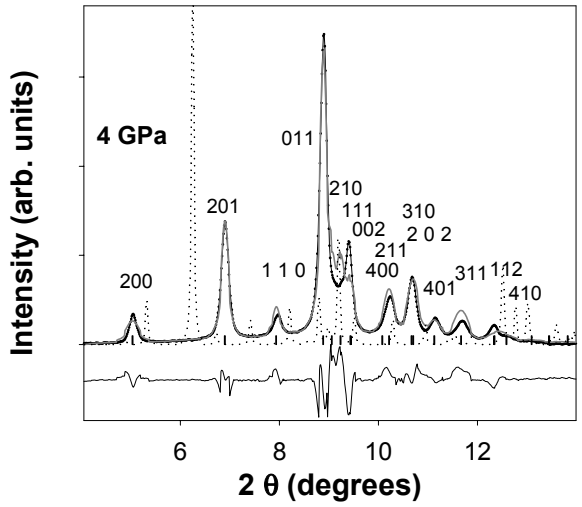

Fig. 5. XRD pattern (λ = 0.4245 Å) of formic acid after unloading from 45 GPa. Solid lines- experiment, gray line- computer generated diffraction pattern for *Pna2₁* structure, dotted line – that for *Pnma* structure [6]. The lower curve in (a) is the fit residual.

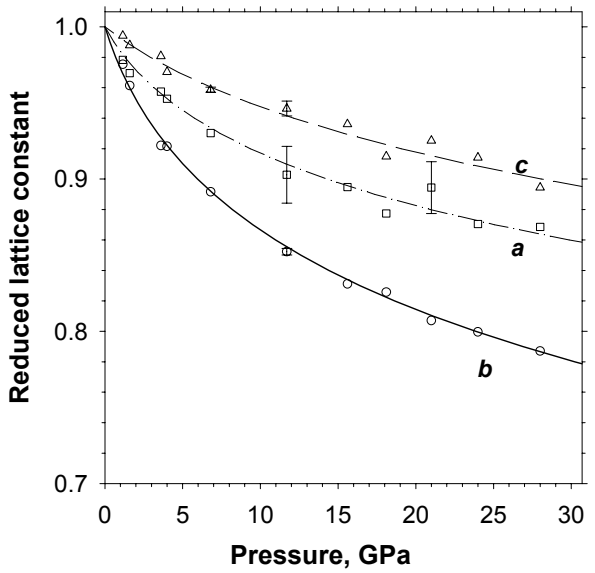

Fig. 6. Reduced lattice constants as a function of pressure.

The XRD patterns at higher pressures show that the crystal structure remains unchanged to at least 30 GPa. We observe peak broadening and an increased deviation between measured and calculated positions of the XRD peaks, which indicate the presence of deviatoric stresses and pressure inhomogeneity. Nevertheless, our data are accurate enough to confirm that formic acid contracts anisotropically with pressure in qualitative agreement with the calculations (Fig. 6). The structurally weakest direction is along the shorter **b**-axis. This means that the molecular planes (which are along 011 and 01^{-}1 diagonals) rotate with pressure and converge faster than other intermolecular distances. Our low-pressure results compare favorably with the results of previous XRD measurements [8], performed to 12 GPa.

We continued our study of formic acid to higher pressures in 2004, and the results will be published in Ref. [10].

Acknowledgments

Use of the Advanced Photon Source was supported by the U.S. Department of Energy, Office of Science, Office of Basic Energy Sciences, under Contract No. W-31-109-ENG-38. We acknowledge help and support of HPCAT. We thank D. Häusermann and M. Somayazulu for technical help. We also thank C. Young for preparation of SrB_4O_7:Sm^{2+} material and D. Hansen for technical help. Use of the HPCAT facility was supported by DOE-BES, DOE-NNSA (CDAC), NSF, DOD – TACOM, and the W.M. Keck Foundation. This work was performed under the auspices of the U. S. Department of Energy by the University of California, Lawrence Livermore National Laboratory under Contract No.W-7405-Eng-48.

Reference list:

[1] H. K. Mao, P. M. Bell, J. W. Shaner, and D. J. Steinberg, J. Appl. Phys., **49**, 3276-3283 (1978).
[2] M. L. Delitsky and A. L. Lane, Journal of Geophysical Research, **107** (E13) 31391-31403 (1998).
[3] A. F. Goncharov, E. Gregoryanz, J.M. Zaug, J.C. Crowhurst, Optical calibration of pressure sensors for high pressures and temperatures, submitted to J. Appl. Phys., 2004.
[4] F. Datchi, R. LeToullec, and P. Loubeyre, J. Appl. Phys. **81**, 3333-3339 (1997).
[5] S. Rekhi, L. S. Dubrovisky, S. K. Saxena, High Pressure-High Temperature **31**, 299-304 (1999).
[6] D. R. Allan and S. J. Clark, Phys. Rev. Lett. **82**, 3464-3467 (1999).
[7] H. Shimizu, Physica **139&140B**, 479-481 (1986).
[8] H. Yamawaki *et al*., in *Science and Technology of High Pressure*, edited by M. H. Manghnani, W. J. Nellis, and M. Nicol (Universities Press, Hyderabad, India, 2000), pp. 125-128.
[9] I. Nahringbauer, Acta Crystallogr., B **34**, 315-319 (1978**)**.
[10] A. F. Goncharov, M. R. Manaa, J. M. Zaug, R. H. Gee, L. E. Fried, W. B. Montgomery, Polymerization of Formic Acid under High Pressure, Phys. Rev. Lett., submitted in 2004, accepted for publication.